TC02-007

Heat Transfer Measurements for a Horizontal Micro-Tube Using Liquid Crystal Thermography

Lap Mou Tam[1,2], Hou Kuan Tam[1*], Afshin J. Ghajar[3], Wa San Ng[1]

[1]Department of Electromechanical Engineering, Faculty of Science and Technology, University of Macau, Taipa, Macau, China

[2]Institute for the Development and Quality, Macau, china

[3]School of Mechanical and Aerospace Engineering, Oklahoma State University, Stillwater, Oklahoma 074078-5016, USA

[*]Author for correspondence. Tel: +853-8397 8012 Fax: +853-2883 8314; Email: hktam@umac.mo

Abstract: In this study, a non-contact liquid crystal thermography (LCT) method was developed for surface temperature measurements on a horizontal 2000μm macro-tube and 1000μm micro-tube. In the single-phase heat transfer experiments, the fully-developed flow heat transfer data were obtained under the uniform wall heat flux boundary condition. In order to reduce the heat loss, the test tube was placed in a vacuum box. For comparison purposes, the tube surface temperatures were also measured using thermocouples (TC). The results showed that the heat transfer coefficient is affected by the vacuum condition (magnitude of vacuum pressure). For the micro-tube, the expected buoyancy effect was not observed in the laminar region when using the LCT method. The increase of heat transfer in the laminar region due to the surface roughness was also observed. In the turbulent region, the LCT heat transfer data trend was close to the classical correlation. For the entire flow regime, the TC heat transfer data trend was much higher than the LCT data trend due to the thermal shunt effect. Our current LCT results when compared with those of Yang and Lin [1] showed slightly higher heat transfer values.

Keywords: liquid crystal thermography (LCT), thermocouple (TC), micro-tube, heat transfer measurement.

1. INTRODUCTION

Due to rapid advancement in fabrication techniques, the miniaturization of devices and components is ever increasing in many applications. Whether it is in the application of miniature heat exchangers, fuel cells, pumps, compressors, turbines, sensors, or artificial blood vessels, it is necessary to understand the fluid flow in micro-scale channels and tubes. Indeed, within this last decade, countless researchers have been investigating the phenomenon of fluid flow in mini-, micro-, and even nano-channels which are widely used in heat exchanger design to get larger surface area per unit volume, higher heat transfer coefficient, and lower thermal resistance. One major area of research in fluid flow in mini- and micro-channels is the heat transfer characteristic. However, the correlations of the conventional forced convection heat transfer have not been solidly verified to work well for predicting the heat transfer coefficient in micro-tubes.

On one hand, researchers [2,3] have found that the heat transfer characteristic to be above the classical laminar region theory. Meanwhile, some [1,4] have reported that heat transfer correlations for conventional sized tubes to be applicable for mini- and micro-tubes. However, many recent experiments on small-sized tubes and channels have observed the heat transfer characteristic to be higher than the classical turbulent region theory for conventional-sized tubes and channels [5,6], and according to Krishnamoorthy et al. [7], the cause of this discrepancy was attributed to the effect of surface roughness, micro-tube diameter and tube surface temperature measurement methods. To understand the heat transfer characteristic, a systematic experimental investigation on the micro-tubes with various surface roughness values, various diameter values and various surface temperature measurement methods are required.

Regarding to the temperature measurement method, thermocouple (TC) is traditionally used for temperature measurement on the macro-tube. However, for the micro-tube, it is too difficult to attach the thermocouple onto the small surface area. Therefore, an alternative non-contact temperature measurement method, liquid crystal thermography (LCT) method was used in this study. The advantage of the LCT is to prevent the thermal shunt effect and surface contact problem caused by TC. The thermal shunt effect is caused by the mass of the thermocouple. When the thermocouple is attached on the heated tube, a portion of energy is taken up by the mass of the thermocouple. Therefore, the actual temperature is slighlty different from the measured temperatrue. The thermal shunt effect is more pronounced for the smaller area such as the micro-tube.

The major objectives of this study are to (1) establish a heat transfer experimental system with LCT temperature measurement; (2) test the LCT temperature measurement with the macro-tube; (3) compare the LCT micro-tube results with the TC results and the existing LCT results.

2. EXPERIMENTAL SYSTEM SETUP

2.1 Experimental test apparatus

The experimentation for this study was performed using a relatively simple but highly effective apparatus. The apparatus used is designed with the intention of conducting highly accurate heat transfer and pressure drop measurements. In this study, only heat transfer measurements were conducted. An overall schematic for the experimental test apparatus is shown in Fig. 1 The apparatus consists of four major components. These are the fluid delivery system, the flow meter banks, the test section assembly, and the data acquisition system. The fluid delivery system consists of a high pressure cylinder filled with

ultra-high purity nitrogen in combination with a stainless steel pressure vessel. After the working fluid passes through the apparatus, it is collected into a sealed container. The working fluid, distilled water is stored in the stainless steel pressure vessel. As the pressurized nitrogen is fed into the pressure vessel, the working fluid is forced up a stem extending to the bottom of the vessel, out of the pressure vessel, and through the flow meter array and test section. Flow rate of the water entering the array is further regulated using a metering valve. Two Coriolis flow meters are necessary in order to accommodate different range of flow rates. After the working fluid passes through the flow meter array, fluid enters the test section assembly. The test section assembly contains the test section as well as the equipment necessary for heating up the test section and the measurement of inlet and outlet fluid temperatures, pressure drop, and top and bottom wall temperatures. In order to reduce the heat loss, the test section assembly was placed in a vacuum box.

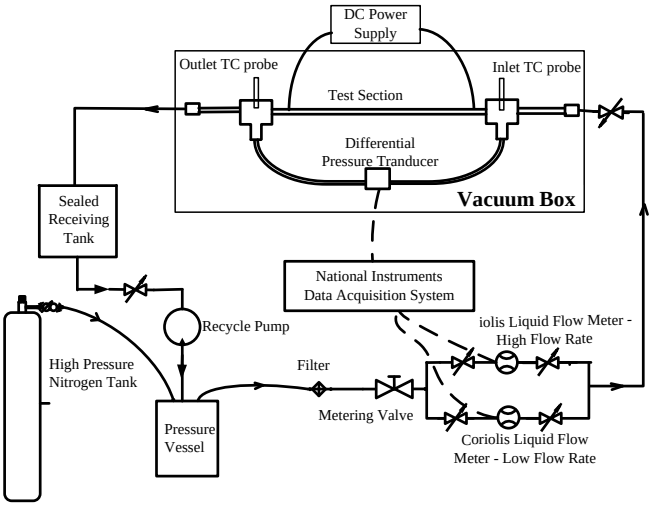

Fig.1 Schematic diagram of experimental setup

Fig.2(a) shows the detailed schematic of the test tube. As shown in the figure, except for the wall temperature measurement station, the whole test tube is covered by the elastomeric insulation material. A pair of electric wires is soldered on to both ends of the test tube. A DC power supply is used to produce the uniform wall heat flux boundary condition. The voltage is measured at the soldered positions of the tube. For the LCT temperature measurement, the black primer and thermochromic liquid crystals (TLCs) are painted onto the wall temperature measurement station. The temperature of TLCs used in this study ranged from 20 ℃ to 40 ℃. As shown in Fig. 2(b), both of the top and bottom wall temperatures were measured. For the LCT temperature measurements, a metallic mirror is placed under the test tube by a horizontal (or view) angle of about 10 degrees. For comparison purposes, at the same station, two Omega self-adhesive Type-T thermocouples (Model no.: SA1XL-T) were placed on the top and bottom walls of the test tube during the experiments.

All the thermocouples were calibrated by a NIST-calibrated thermocouple probe (±0.22 ℃) and an Omega HCTB-3030 constant temperature circulating bath. Therefore, the temperature sensors are as accurate as ±0.22 ℃. Furthermore, the LCT temperature measurement system was calibrated by the constant temperature calibration box. The test tube with TLCs painting, the heating wire and the reference thermocouples were arranged in the calibration box. The temperature inside the box can be controlled from 20 ℃ to 40 ℃ and maintained within ±0.22 ℃. With different temperatures, different hue values of the TLC on the test tube can be observed. Fig. 3 shows the relationship of the hue value and the calibration temperature. For data reduction, cubic polynomial correlations for the top and bottom wall temperature measurements were established. The maximum standard deviation between the measured values and the correlated values were less than 2.41%.

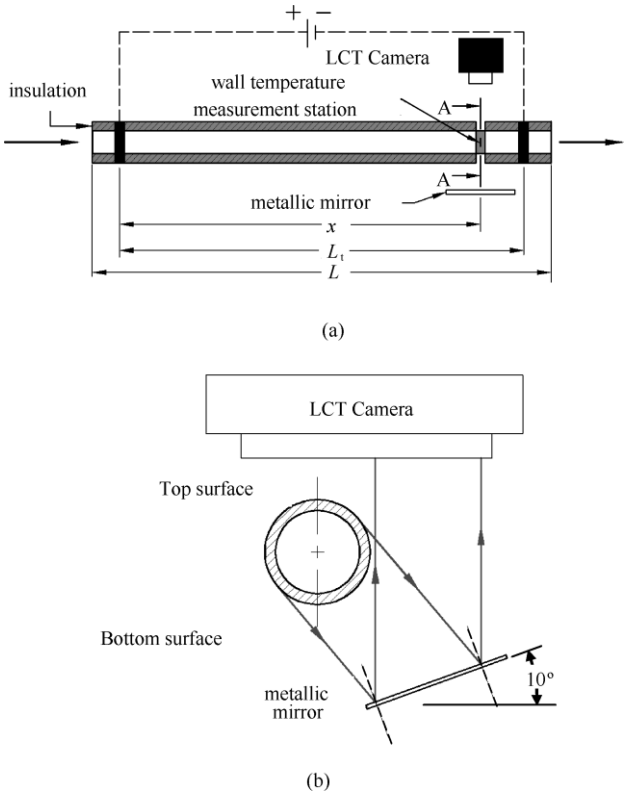

Fig.2 (a) Test section; (b) Sectional view of the wall temperature measurement station

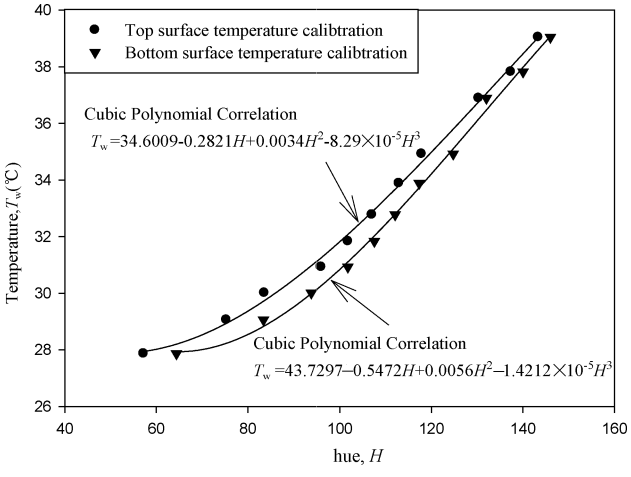

Fig.3 The relationship between the caliberated top and bottom wall temperatures and their corresponding hue values

In this study, two stainless steel tubes (2000μm macro-tube and 1000μm micro-tube) were used. The tube diameter was accuractely measured by the the scanning electron microscope (SEM). Fig. 4 shows the SEM measurements for the two test tubes. For measuring the inner surface roughness, a Stylus 3D Surface Profilometer was used. The surface roughness values and the tubes dimensions are summarized in Table 1.

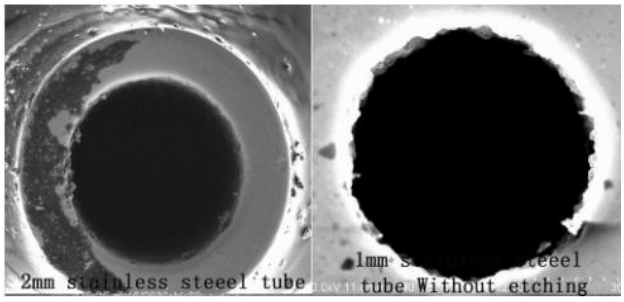

(a) (b)

Fig. 4 SEM measurement of the stainless steel tubes: (a) 2000μm tube; (b) 1000μm tube

Table 1. The specifications of the test tubes

	2000μm Macro-tube	1000μm Micro-tube
Outer diameter, d_o(μm)	3180	1580
Inner diameter, d_i(μm)	2000±32	1000±14
Surface Roughness, *Ra* (μm)	4.27	3.29
Roughness height to inner dimeter ratio, ε/ d_i	0.00213	0.00329
Tube length, *L*(mm)	500	300
Heating length, L_t (mm)	450	275
Dimensionless axial distance for wall temperature measurement, x/d_i	200	240

2.2 Data reduction and uncertainty analysis

Regardless of the peripheral wall temperature measured by LCT or TC, the inside wall temperatures and the local heat transfer coefficient were calculated by the method shown in [8]. In these calculations, the axial conduction was assumed negligible (*RePr* > 2,800 in all tests), but peripheral and radial conduction of heat in the tube wall were included. In addition, the bulk fluid temperature was assumed to increase linearly from the inlet to the outlet. Also, the dimensionless numbers, such as Reynolds, Prandtl, Grashof, and Nusselt were computed by the computer program developed by [8].

The Reynolds number range for this study was from 700 to 15,000. The inlet and outlet temperature difference was round 5℃ for the whole Reynolds number range. The uniform wall average heat flux for the experiments ranged from 16 to 200 W/m^2. Heat balance errors were calculated for all experimental runs by taking a difference between two methods of calculating the heat addition. The product of the voltage drop across the test section and the current carried by the tube was the primary method, while the fluid enthalpy rise from inlet to outlet was the secondary method. In all cases the heat balance error was less than ±8%. The primary method is the one used in the computer program [8] for all heat flux and heat transfer coefficient calculations. The uncertainties for the experiments are listed in Table 2.

Table 2. Uncertainties for the experiments

Measured variables		Calculated varaiables	
Variable	Uncertainty	Variable	Uncertainty
Temperatures	0.22 ℃	Heat transfer coefficient (*h*)	±22%
Mass flow rate	0.5% of full rage	Heat transfer coefficient (*Nu*)	±22%
Density	0.2 kg/m^3		
Diameter	0.001mm		
Length	0.1mm		
Voltage	1%		
Current	1%		

3. RESULTS AND DISCUSSION

To verify the new experimental setup, experiments for 2000μm stainless steel tube were conducted first. Fig. 5 shows the comparison of 2,000μm tube heat transfer data (measured by TC and LCT) with the data of Ghajar and Tam [9] for a 15,800μm stainless steel tube with a square-edged inlet. The square-edged inlet data is used because the inlet of this study is also similar. Since the deviations between the three data sets are below ±10%, the experimental setup for the heat transfer measurements and the heat transfer data are confirmed to be reliable. It should be noted that the parallel shift from the classical fully developed value (*Nu* = 4.364) for the uniform wall heat flux boundary condition in the laminar region is due to the buoyancy effect.

During the experiments, the effect of magnitude of the vacuum pressure on the heat transfer data was observed. Fig.6 shows this effect on the heat transfe data for the 1,000μm tube. From the figure, it can be observed that the highest degree of vacuum (lowest vacuum pressure of 260 mmHg) provided the expected heat transfer charactertics similar to those observed in Fig. 5. For the lower degrees of vacuum (high vacuum pressures or no vacuum), the heat transfer data became scattered and did not follow the expected pattern. Therefore, for the micro-tube studies, the higher degree of vacuum condition (low vacuum pressure) is recommended.

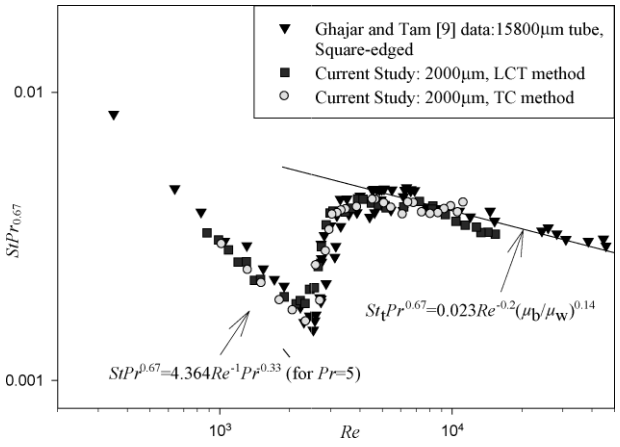

Fig.5 Comparison of the current 2000μm tube heat transfer data with the experimental data of Ghajar and Tam [9] at x/d_i of 200

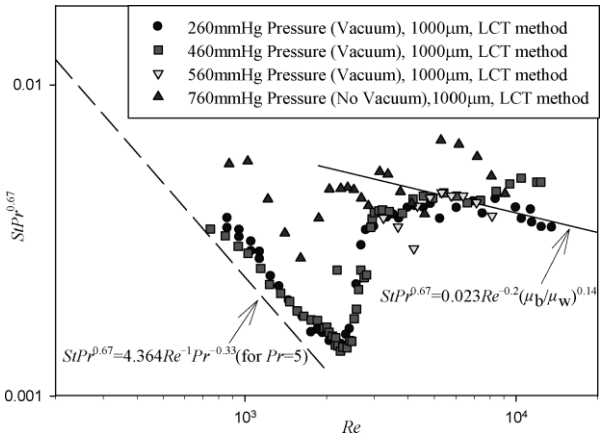

Fig.6 Comparison of heat tranfser characteristics with different vacuum conditions for the 1000μm tube

After the verification of the experimental setup, the heat transfer measurements under unifrom wall heat flux boundary conditions for the 1,000μm micro-tube were conducted. Fig. 7 shows the heat transfer characteritics of the micro-tube with the two temperature measurement methods (TC and LCT). In the laminar region, the LCT heat transfer data show a parallel shift from the classical fully developed value of Nu = 4.364 for the uniform wall heat flux boundary condition. However, this is not due to the buoyancy effect. According to the experimental data, the heat transfer coefficient ratio at the top and bottom walls (h_t /h_b) is higher than 0.8. Referring to Ghajar and Tam [9], the buoyancy effect exists when the heat transfer coefficient ratio at the top and bottom walls (h_t /h_b) is less than 0.8. Referring to Kandlikar et al. [2], the increase of heat transfer in the laminar region can be caused by the inner surface roughness. Therefore, in our case, the increase of heat transfer for the micro-tube is due to the surface roughness. In the transition and turbulent regions, the LCT heat transfer trend is similar to the macro-tube. Especially, the LCT turublent heat transfer data follows the macro-tube correlation of Sieder and Tate [10]. Therefore, the roughness does not have a significant effect on the 1,000μm micro-tube heat transfer in the transition and turbulent regions. In comparing the LCT heat transfer data with the TC heat transfer data, the entire TC heat transfer trend is higher than the LCT. Especially, in the turbulent region, the TC heat transfer data trend does not follow the macro-scale turbulent correlation. Referring to Yang and Lin [1], this is due to the thermal shunt error caused by using thermocouples for temperature measurements.

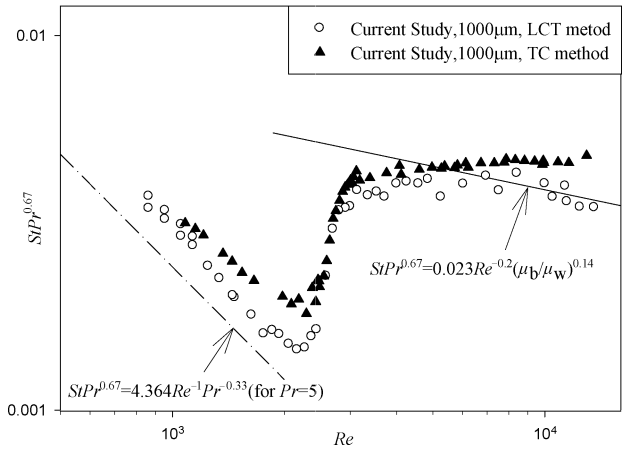

Fig.7 Comparison of the 1000 μm tube data measured by LCT and TC methods

Fig. 8 shows the comparion of the current heat transfer data (measured by LCT and TC) with the heat transfer data (measured by LCT) of Yang and Lin [1]. As shown in the figure, the current TC heat transfer data is higher than the current LCT data and the LCT data of Yang and Lin [1]. In the laminar region, data of [1] is very close to the classical laminar line (Nu = 4.364). It appears that their data is not influenced by any buoyancy and roughness effects. In their study, surface roughness value of the stainless steel tube was 1.4μm. Compared to the surface roughness of the current 1000μm tube (Ra = 3.29μm), their surface roughness value is much smaller. Therefore the increase of the heat transfer in the laminar region for the current study can be explained by the surface roughness effect. In the turbulent region, the current LCT data follows the well-established macro-tube correlation of Gnielinski [11]. However, Yang and Lin's turbulent data is lower than the current LCT data. This could be due to the camera setting for the LCT measurements and the heat loss effect. In their study, only one side of the tube wall temperature was captured by the LCT camera. Furthermore, from their reported work it appears that they did not control/prevent the heat loss from their heated test section by either insulating it or placing it in a vacuum box.

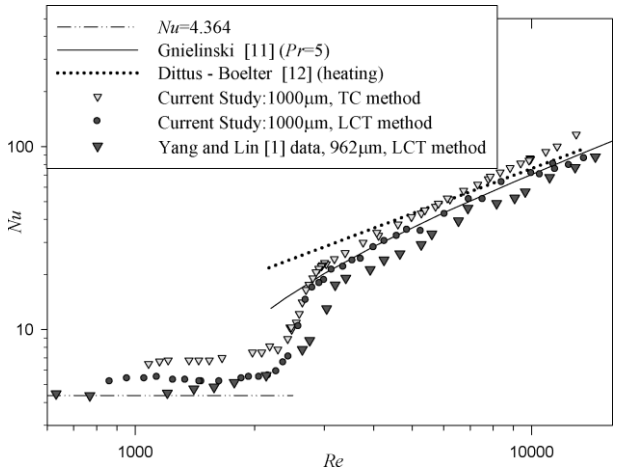

Fig.8 Comparison of current TC and LCT results with the LCT results of Yang and Lin [1]

4. CONCLUSIONS

In this study, the heat transfer experimental setup with LCT temperature measurement for the macro- and micro-tubes was introduced. The experimental setup was verified for the macro-tube under the vacuum condition.

For the micro-tube using the LCT measurement, it could be concluded that (1) the heat transfer coefficient was affected by the magnitude of the vacuum pressure; (2) the buoyancy effect was not observed in the laminar region; (3) the LCT turbulent data trend was close to the classical correlations; (4) the TC heat transfer data trend was much higher than the LCT data trend; and (5) the current LCT results were slightly higher than the LCT results of Yang and Lin [1].

Acknowledgments

This research is supported by the Fundo para o Desenvolvimento das Ciencias e da Tecnologia under project no. 033/2008/A2 and the Institute for the Development and Quality, Macau.

References

[1] C.-Y. Yang, T.-Y. Lin, Heat transfer characteristics of water flow in micro-tubes, Experimental Thermal and Fluid Science 32 (2007) 432-439.

[2] S. G. Kandlikar, S. Joshi, S. Tian, Effect of surface roughness on heat transfer and fluid flow characteristics at low reynolds numbers in small diameter tubes, Heat Transfer Enginnering 24 (2003) 4-16.

[3] A. Bucci., G. P. Celata, M. Cumo, E. Serra, and G. Zummo, Water single phase fluid flow and heat transfer in capillary tubes, *First International Conference on Microchannel and Minichannels*, 24-25 April (2003) 319-226, Rochester, New York, USA.

[4] C.-Y. Yang, T.-Y. Lin, An experimental investigation on forced convection heat transfer performance in micro tubes by the method of liquid crystal thermography, International Journal of Heat and Mass Transfer 50 (2007) 4736-4742.

[5] Z. G. Liu, S. Q. Liang, and M. Takei, Experimental Study on Forced Convective Heat Transfer Characteristics in Quartz Micro-Tube, International Journal of Thermal Science, 46 (2007) 139-148.

[6] Y. Zhao, and Z. Liu, Experimental Studies on Flow Visualization and Heat Transfer Characteristics in Microtubes, *13th International Heat Transfer Confernce*, 13-18 August 2006, Sydney, Australia.

[7] C. Krishnamoorthy, R. P. Rao, A. J. Ghajar, Single-phase heat transfer in micro-tubes, *Proceedings of HT2007, ASME-JSME Thermal Engineering Summer Heat Transfer Conference*, 8-12 July 2007, Vancouver, British Columbia, Canada.

[8] A. J. Ghajar and J. Kim, Calculation of local inside-wall convective heat transfer parameters from measurements of the local outside-wall temperatures along an electrically heated circular tube, Heat Transfer Calculations, edited by Myer Kutz, McGraw-Hill, New York, NY, (2006) 23.3-23.27.

[9] A. J. Ghajar, L. M. Tam, Heat transfer measurements and correlations in the transition region for acircular tube with three different inlet configurations, Experimental Thermal and Fluid Science 8 (1994) 79-90.

[10] E. N. Sieder, and G. E. Tate, Heat Transfer and Pressure Drop in Liquids in Tubes, International Journal of Chemical Engineering 28 (1936) 1429-1435.

[11] V. Gnielinski, New equation for heat and mass transfer in turbulent pipe and channel flow, International Journal of Chemical Engineering 16 (1976) 359-368.

[12] F. W. Dittus, and L. N. K. Boelter, Heat transfer in automobile radiators of the tubular type, University of California, Berkeley, Publications on Engineering 2 (1930) 443-461.

Nomenclature

c_p specific heat of the test fluid evaluated at T_b, [J/(kg·K)]
d_i inside diameter of the test section, (m)
d_o outside diameter of the test section, (m)
H hue value, dimensionless
h local average or fully developed peripheral heat transfer coefficient, [W/(m^2·K)]
h_t local peripheral heat transfer coefficient at the top of the tube, [W/(m^2·K)]
h_b local peripheral heat transfer coefficient at the bottom of the tube, [W/(m^2·K)]
k thermal conductivity of the test fluid evaluated at T_b, [W/(m·K)]
L total length of the test section, (m)
L_t heating length of the test section, (m)
Nu local average or fully developed peripheral Nusselt number (= h·d_i /k), dimensionless
Pr local bulk Prandtl number (=c_p·μ_b/k), dimensionless
Ra surface roughness, (μm)
Re local bulk Reynolds number (=ρ·V·d_i /μ_b), dimensionless
St local average or fully developed peripheral Staton number [=Nu / (Pr·Re)], dimensionless
T_b local bulk temperature of the test fluid, (℃)
T_w local inside wall temperature, (℃)
V average velocity in the test section, (m/s)
x local axial distance along the test section from the inlet, (m)

Greek letters

μ_b absolute viscosity of the test fluid evaluated at T_b, (Pa·s)
μ_w absolute viscosity of the test fluid evaluated at T_w, (Pa·s)
ε roughness height, (μm)
ρ density of the test fluid evaluated at T_b, (kg/m^3)

Subscripts

l laminar
t turbulent

Abbreviations

LCT Liquid Crystal Thermography
TC Thermocouple
SEM Scannnig Electron Microscope